August 27-31, 2023
FLORENCE - ITALY
ICWE 16
16th International Conference on Wind Engineering

# Pedestrian-level strong wind distribution within a simplified block array determined by particle image velocimetry

Chiyoko Hirose[1], Naoki Ikegaya [1]

[1]*Faculty of Engineering Sciences, Kyushu University, Kasuga, Japan, chiyoko_ikgy@kyudai.jp, ikegaya@cm.kyushu-u.ac.jp*

**SUMMARY:**
The gust events at the pedestrian level within an urban canopy layer are mostly unpredictable because of the complexity of flow fields due to the aerodynamic effects from surrounding buildings. In this study, therefore, two velocity components within a simplified urban canopy layer were measured using time-resolved particle image velocimetry (PIV) to investigate the relationships between the gust distributions and the flow patterns around buildings. The new laser-camera system realized by inserting a laser optics system into a block neighbouring measurement area could successfully capture the velocity fields within a simplified urban-like array. Accordingly, we discussed the spatial distribution of gust indices such as gust factor (GF), peak factor (PF) and integral time scale. This study enabled us to understand the spatio-temporal features of the gust events at the pedestrian level.

*Keywords: Urban canopy flow, Power spectral density, Gust wind*

## 1. INTRODUCTION

The accurate prediction of extreme wind events (*e.g.*, the gust or stagnation of the contaminated air) in an urban area is challenging due to the complex flow fields characterised by the broad-ranging time variations as well as three-dimensional structures. Based on the social requests for realizing comfortable and safe wind environment in urban areas, enormous numerical studies dealing with the pedestrian-level wind (PLW) have reported the stochastic features of turbulent flow around buildings based on the probability density functions (PDFs) of wind speeds and velocity components in recent years (Kawaminami et al., 2018; Wang and Okaze, 2022). On the other hand, the experimental studies using PIV for the PLWs in horizontal plains, which can provide persuasive validation data for numerical studies, have been quite limited due to the methodological difficulties for capturing the velocity fields in the canopy areas sheltered by the surrounding blocks A pioneering study by Hirose et al., 2022 has successfully exhibited the distributions of evaluation indices for the pedestrian wind environment (such as gust factor (GF) and peak factor (PF)) within un urban canopy layer based on PIV measurements by optimizing the laser and camera systems to capture the velocity fields under the sheltered conditions. Although they showed numerous instantaneous and averaged velocity components as well as stochastic natures of the gust and peak factors, the relationships between the gust distributions and flow patterns around urban buildings have not been well understood yet. Thus, in this study, we expanded the velocity fields within the canopy layer based on the time-resolved PIV measurements to determine the velocity fields in a horizontal plane within an urban-like canopy array (Hirose et

al., 2022) and scrutinized the spatio-temporal features of gust events intermittently happened at the pedestrian level within the urban canopy layer.

## 2. METHOD

### 2.1. Experimental setup

Wind tunnel experiments using PIV were conducted in a closed-circuit wind tunnel at the laboratory of the Interdisciplinary Graduate School of Engineering Sciences, Kyushu University, Japan. The sizes of the test sections were 5.0 m, 1.5 m, and 1.0 m in the streamwise ($x$), spanwise ($y$), and vertical ($z$) directions, respectively. Here, their corresponding velocity components are denoted by $u$, $v$, and $w$, respectively. Within the entire test section shown in Fig. 1 (a), solid cubes 0.1 m (=$H$) on a side were arranged in a staggered layout with a packing density of 25%, which configured 33 and 14 rows in the $x$ and $y$ directions, respectively. The target area was located in the spanwise center and 27 rows downstream from the upstream-side edge as shown by the dotted red lines in Fig. 1 (b). In this study, a laser camera system (including optical devices such as the continuous-wave laser (Verdi G12) and high-speed camera (Phantom T1340)) was installed beneath the wind-tunnel floor to measure the velocity field within the target area. The measurement area was located at the wake region of the upstream building. The particle reflection images in the target area of 0.1 × 0.1 m$^2$ ($= H \times H$) were captured as 1024 × 1024 pixels. According to the specifications and data capacity of the high-speed camera, a flame rate of 2000 fps and exposure period of 500 μs were employed. Under these conditions, the acquisition durations reached 10s. Two trials were repeated under the same measurement conditions. During each PIV measurement, a reference wind speed at $z = 5H$ above the target area $u_{ref}$ [m/s] was measured using a pitot static tube connected to a manometer (DPC-500N12) and data logger (GL900).

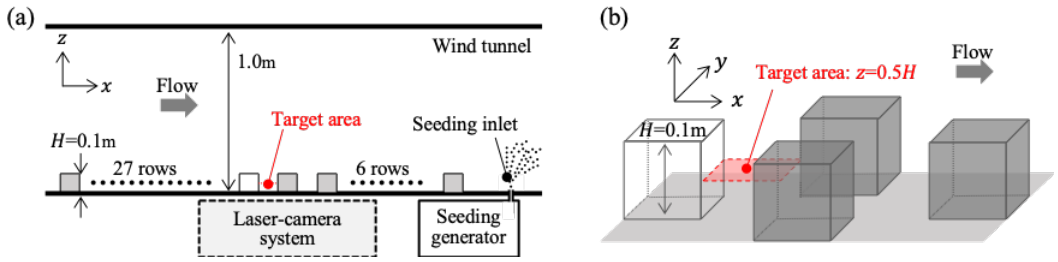


**Figure 1.** Schematics of (a) experimental setups and (b) target area.

### 2.2. Data Analysis

As Ikegaya et al., 2019 discussed, the frame rates of the PIV using CW laser is not consistent with the effective data frequency because of the limitation determining the interrogation window size and mean particle displacement between two frames. Therefore, the spectral density for streamwise velocity $u$ was calculated by means of the fast Fourier transform to consider the effective frequency caused by PIV measurements. In Fig. 2, the horizontal and vertical axes indicate frequency $f$ [Hz] and power spectral density for $u$ denoted by $S_u(f)$ (scaled by standard deviation of $u, \sigma_u$ [m/s], and $f$), respectively. The raw data and low-pass filtered data with 250 Hz in each trial obtained at position-A $(x, y, z)$= $(0.2H, 0.8H, 0.5H)$ and position-B $(0.8H,\ 0.2H, 0.5H)$ are provided in Fig. 2(a) and (b), respectively. In addition, the dotted line in each figure represents the von Karman spectrum for $u$ (von Karman, 1948) which is based on the

integral time scale $\tau$ [s] calculated by Eqs. (1)-(2) in each trial.

$$\tau = \int_0^{t_0} R(\Delta t) d\Delta t. \tag{1}$$

$$R(\Delta t) = \frac{\overline{v_a'(t) v_a'(t+\Delta t)}}{\sigma_{v_a}^2}, \tag{2}$$

where $t_0$ [s] is the time when the correlation coefficient $R(\Delta t)$ becomes 0.1, $v_a$ $(= \sqrt{u^2 + v^2})$ [m/s] represents the horizontal wind speed, $v_a'(t)$ $(= v_a(t) - \overline{v_a})$ [m/s] is the time fluctuation of $v_a$, $\sigma_{v_a}$ [m/s] indicates the standard deviation of $v_a$, and the overbar indicates the temporal averaging operation. According to Fig. 2, we can confirm that the raw data in two trials (*i.e.*, data-1 and data-2 in Fig. 2) are basically consistent with each other at both positions, and the low-pass filtering operation reasonably works in both cases for eliminating the white noise observed over 250 Hz in raw data. On the other hand, we can observe that the discrepancies between the von Karman spectrum and results of position-A (Fig. 2(a)) are more obvious than those at position-B (Fig. 2(b)). Due to the significant effects from the buildings on the flow field, the spectral density at position-A is considered to exceed the von Karman spectrum within the high frequency region.

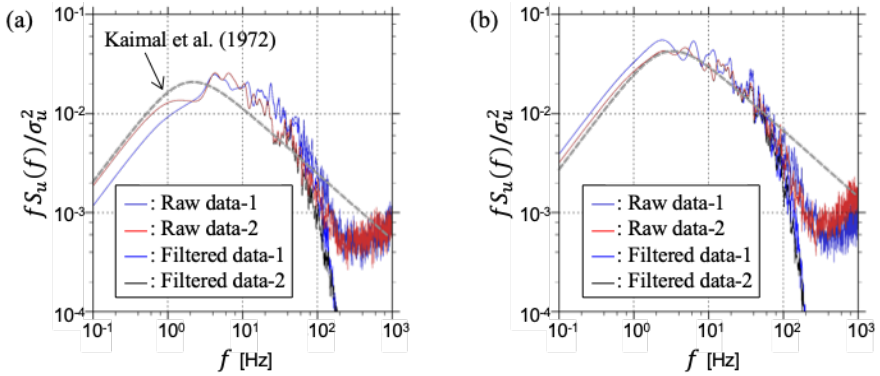


**Figure 2.** Power spectral density $S_u$ distributions at positions (a) A and (b) B. Raw data indicates the $S_u$ determined by the time series data with 2000 Hz, whereas filtered data means 250 Hz lowpass filtered data.

## 3. GUST DISTRIBUTIONS

To understand the spatio-temporal features of gust wind in the target area, the distributions of GF, PF and $\tau$ are investigated in Fig. 3. The GF and PF are calculated by Eqs. (3) and (4), respectively, for each trial, and the ensemble averages of two trials are provided in Fig. 3.

$$PF = \frac{\widehat{v_a} - \overline{v_a}}{\sigma_{v_a}}, \tag{3}$$

$$GF = \frac{\widehat{v_a}}{\overline{v_a}}, \tag{4}$$

where the hat indicates the maximum value of a variable during 10 s. In Fig. 3, the arrow shows mean velocity vector $(\overline{u}, \overline{v})$, and its length represents the magnitude of $(\overline{u}, \overline{v})$, $U$, normalized by $u_{ref}$. As shown in Fig. 3 (a) and (b), the distributions of $GF$ and $PF$ tend to be consistent with each other, which show high values in the wake region where the aerodynamic effects from the

building model at the upstream side are significant and low values at the high-speed flow area resulting from the separated flow. In addition, $\tau$ in the wake region tends to be small (Fig. 3(c)), where both $GF$ and $PF$ are observed to be large. These trends seem reasonable as referring to the prediction model of the peak values considering the turbulent time scale (Davenport, 1964) since more eddies, which increase the randomness of the flow field (*i.e.*, $GF$ and $PF$), can pass through during a certain period as the integral time scale are smaller.

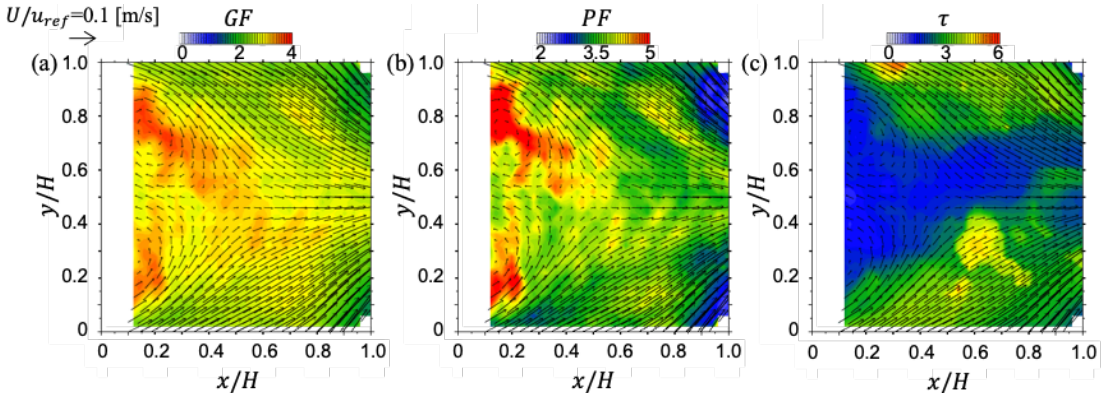


**Figure 3.** Distributions of (a) gust factor $GF$, (b) peak factor $PF$, and (c) integral time scale $\tau$ in the wake of a block in the urban array. The white areas indicate the data missing regions due to the block.

## 4. CONCLUSION

In this study, two velocity components within an urban canopy layer were measured using time-resolved PIV by inserting a laser optics system into a neighbouring block. We examined the spectral density distribution to validate the applicability of the PIV method to the current simplified urban block array, and investigated the distributions of gust factor, peak factor, and integral time scale for eddies to understand the spatial and temporal features of the occurrence of gust events at the pedestrian level in an urban canopy layer.


### ACKNOWLEDGEMENTS

This study was partially supported by a Grant-in-Aid for Scientific Research from JSPS, Japan, KAKENHI [grant numbers JP21K18770, JP21K14305] and JST FOREST program [grant number JPMJFR205O].


### REFERENCES


Davenport, A.G., 1964, Note on the distribution of the largest values of a random function with application to gust loading, Procs. of the institution of Civil Engineers, 28, 2, 187-196.

Hirose, C., Nomichi, T., Ikegaya, N., 2022. Distributions of gust and peak factors at a pedestrian level in a simplified urban canopy obtained by particle image velocimetry. Building and Environment, 222, 109350.

Ikegaya, N., Hasegawa, S., Hagishima, A., 2019, Time-resolved particle image velocimetry for cross-ventilation flow of generic block sheltered by urban-like block arrays. Building and Environment, 147, 132-145

Kawaminami, T., Ikegaya, N., Hagishima, A., Tanimoto, J., 2018. Velocity and scalar concentrations with low occurrence frequencies within urban canopy regions in a neutrally stable shear flow over simplified urban arrays. Journal of Wind Engineering and Industrial Aerodynamics, 182, 286–294.

Wang, W. and Okaze, T., 2022. Statistical analysis of low-occurrence strong wind speeds at the pedestrian level around a simplified building based on the Weibull distribution. Building and Environment, 209, 108644.

von Karman, T., 1948. Progress in the statistical theory of turbulence. Proc. Natl. Acad. Sci. U.S.A. 34 (11), 530-539.